

ISL72027SEH, ISL72027BSEH

Single Event Effects (SEE) Testing

TR018

Rev 2.00

November 17, 2016

Introduction

The intense proton and heavy ion environment encountered in space applications can cause a variety of Single Event Effects (SEE) in electronic circuitry, including Single Event Upset (SEU), Single Event Transient (SET), Single Event Functional Interrupt (SEFI), Single Event Gate Rupture (SEGR), and Single Event Burnout (SEB). SEE can lead to system-level performance issues including disruption, degradation, and destruction. For predictable and reliable space system operation, individual electronic components should be characterized to determine their SEE response. This report discusses the results of SEE testing performed on the [ISL72027SEH](#) CAN transceiver. This report also applies to the [ISL72027BSEH](#) (with the “B” suffix).

Product Description

The ISL72026SEH, ISL72027SEH, and ISL72028SEH are a family of radiation tolerant Controller Area Network (CAN) bus transceivers. These parts are designed to meet ISO11898-2 physical layer specifications. They are fabricated in Intersil's proprietary BCD SOI process with deep trench isolation. The ISL7202xSEH parts are bond options of the same silicon die. The “B” suffix parts are also represented by the SEE results reported here. Further description and explanation of the differences between the parts can be found in the datasheets.

Related Literature

- For a full list of related documents please visit our web pages
 - [ISL72027SEH](#) product page
 - [ISL72027BSEH](#) product page

SEE Test Objectives

The ISL72027SEH was tested to determine its susceptibility to destructive single event effects (collectively referred to as SEB) and to characterize its Single Event Transient (SET) behavior over various operating conditions. Since the family of parts utilizes the same silicon with only bond-out options, it was determined that testing the ISL72027SEH would serve to characterize all three parts. More description of the part differences follows in the next two paragraphs. Thereafter, the report will refer only to the ISL72027SEH with the understanding that the results apply equally to the other two members of the family, the ISL72026SEH and ISL72028SEH.

The ISL72026SEH and ISL72027SEH differ in that the Loopback (LBK) command input of the ISL72026SEH is not bonded out in the ISL72027SEH. Instead, V_{REF} is bonded out in the ISL72027SEH. All other pins and functions are the same. Since the LBK has an internal pull-down, the LBK function is constantly deasserted in the ISL72027SEH, but the LBK circuitry is fully active and available to SEE events that could cause LBK to be momentarily asserted. On the other hand, the V_{REF} circuitry is fully active in the ISL72026SEH, however, is simply not brought out to the outside world. Consequently, all that is lost in testing the ISL72027SEH rather

than the ISL72026SEH is that the part is not tested while in the LBK mode. Since this is a diagnostic mode and is expected to be active only a very small fraction of the operational life, it does not seem to represent a statistically important mode for SEE events. The jeopardy is that an SET could momentarily take the part out of LBK, however, this would be an extremely unlikely event if LBK is not a dominant operational mode.

The ISL72028SEH differs from the ISL72027SEH in that the RS pin, when pulled to VCC, can invoke a Low Power Shutdown (LPSD) mode rather than the Listen Mode (LM) of the ISL72027SEH. Both circuits are operational in both parts; however, a pin control is only effective according to the part type. So, if either the LM or LPSD can be activated by SEE, either circuit would be susceptible. What is lost in testing the ISL72027SEH is the event where an SET triggers the ISL72028SEH out of LPSD. Such an event would be of little interest to the operation of the system, so it is not perceived as an important omission.

SEE Test Facility

Testing was performed at the Texas A&M University (TAMU) Radiation Effects Facility of the Cyclotron Institute heavy ion facility. This facility is coupled to a K500 superconducting cyclotron, which is capable of generating a wide range of particle beams with the various energy, flux, and fluence levels needed for advanced radiation testing. The Devices Under Test (DUTs) were located in air at 40mm from the aramica window for the ion beam. The ion LET values are quoted at the DUT surface. Signals were communicated to and from the DUT test fixture through 20 foot cables connecting to the control room. Testing was carried out over four trips to TAMU, on November 7 and 8, 2014, December 1, 2014, March 18, 2015, and June 2, 2015.

SEE Test Set-Up

SEE testing was carried out with the samples in an active configuration. The schematic of the ISL72027SEH SEE test fixture used in 2015 is shown in [Figure 1, on page 2](#). This schematic shows direct access to the CANH/CANL bus pins for monitoring and indirect access through 30Ω resistors for biasing. These resistor feeds were not there in the 2014 testing so that bus bias and monitor were done through the same lines. The cabling connected to the CANH/CANL pins present 700pF to GND due to the 20 foot cable connecting the DUT to the oscilloscopes in the control room for SET testing. Other supplies and signals indicated by arrows were also cabled to the control room.

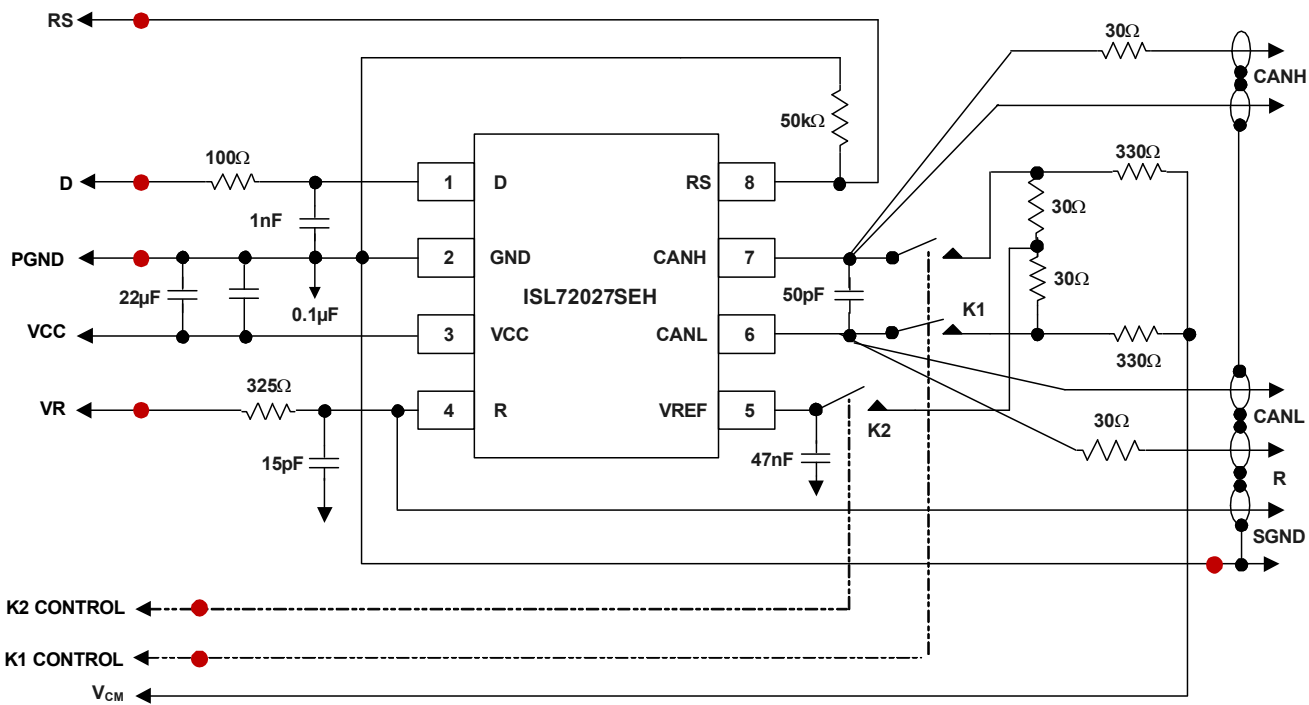
Two instantiations of the schematic on a single board allowed two ISL72027SEH to be simultaneously irradiated for SEE testing. The two parts were monitored separately. Parts were packaged in the flatpack and had their lids removed for the SEE testing. For SEB, the parts' key currents and V_{REF} voltage were monitored before and after irradiation to determine if any change had been induced. For SET testing, the outputs of the

CAN bus (CANH and CANL) and the received signal, R, were monitored. In static SET testing any change in R triggered an oscilloscope capture. In dynamic SET testing the bus and receiver were monitored for changes in the bit stream resulting from the provided input signal. For dynamic inputs, if the received bit stream, R, deviated from its nominal duty cycle (nominally 50%, triggered at either $\pm 10\%$ from there) an oscilloscope capture was triggered and the event was stored for later review.

The parts tested in 2014 came from lot J66594.1 (part # B2330-X18). The parts tested were all modified in metal by Focused Ion Beam (FIB) techniques to correct two problems seen on these first parts:

- Receiver transition glitches
- Low CANH/CANL breakdowns

These changes are metal fixes instituted in the final product so the FIB modified units accurately represent the final product. The parts tested in 2015 came from lot J66594.2 (part # B2330-X28) and had the metal changes incorporated in manufacture that were previously done by FIB. The latter parts are the production product.



Note: The V_{REF} can be monitored at the external connection V_{CM} when K2 is closed and K1 is open

FIGURE 1. Schematic of the ISL72027SEH SEE test configuration used in 2015. Connection to CANH/CANL through resistors allows setting bus voltage while direct connections allow monitoring bus voltage at the unit.

March 2015 SEB Testing of the ISL72027SEH CAN Transceiver

Four units of the ISL72027SEH were irradiated for the purposes of destructive SEE (SEB) testing. Four currents and the V_{REF} output voltage were monitored as in [Table 1 on page 4](#) to determine if permanent change was induced during irradiations. After initial measurements according to [Table 1](#), a set of six irradiations was performed as listed in [Table 2 on page 4](#). Each irradiation was done with 2.114GeV Pr (praseodymium) at 10° incidence for a surface LET = $60\text{MeV} \cdot \text{cm}^2/\text{mg}$ to a fluence of 5×10^6 ion/ cm^2 per irradiation at fluxes under 2.5×10^4 ion/ $(\text{cm}^2 \cdot \text{s})$. The ICC and ICM were measured before and after each irradiation to look for indications of damage in changes of those parameters. At the end of the set of six irradiations the parameters in [Table 1](#) were again measured to look for any changes.

The 50kHz data signal allowed for the common-mode voltage to dominate the bus pins during the recessive periods but still exercised switching conditions. [Figures 2](#) and [3](#) offer examples of the timing requirements of the 50kHz input signal. The 47nF capacitor on V_{REF} and the resistors in the V_{CM} path were what set the time constant of the common-mode voltage. The complement of six irradiations accounted for 58krad of total

dose when combined with a similar set done with common-mode voltages of $\pm 17\text{V}$ before moving on to the $\pm 18\text{V}$ set reported here. The device case temperature was heated to $+125^\circ\text{C} \pm 10^\circ\text{C}$ for the irradiations with a thin film heater mounted on the board. The heater setting was calibrated with a thermocouple on the case at the Intersil lab before traveling to TAMU. At TAMU the heater was set to the predetermined setting to yield the $+125^\circ\text{C}$ case temperature. At the end of the six irradiations outlined in [Table 2](#), the monitor parameter measurements of [Table 1](#) were repeated to check for changes.

[Table 3 on page 4](#) presents the log of the ICC and ICM measurements made for each irradiation run at the conditions described in [Table 2](#). The same data is presented in [Table 4 on page 5](#) as the percentage change in the measured currents. Changes of less than 5% were considered to be within measurement error and not interpreted as indicative of damage. [Table 5 on page 5](#) presents the measurements of monitor parameters in [Table 1](#) made both before and after the groupings of six irradiations. [Table 6 on page 5](#) presents the monitor data of [Table 5](#) as percentage change. Again, changes of 5% or less are viewed as within measurement error. On the basis of these tests, the part is found to be free of damaging SEE up to LET = $60\text{MeV} \cdot \text{cm}^2/\text{mg}$ (Pr at 10° incidence) and the conditions listed in [Table 2](#).

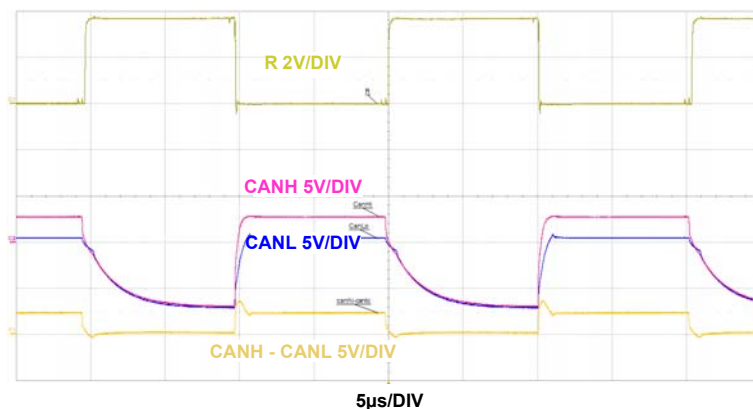


FIGURE 2. Example of CANH/CANL switching at 50kHz, $V_{CC} = 3.6\text{V}$ and a common-mode of -7V . Time allows recessive state to stabilize at -7V for the CANH/CANL lines. Time scale is $5\mu\text{s}/\text{Div}$, and the vertical axis is $2\text{V}/\text{Div}$ for the upper plot and $5\text{V}/\text{Div}$ for the lower three plots.

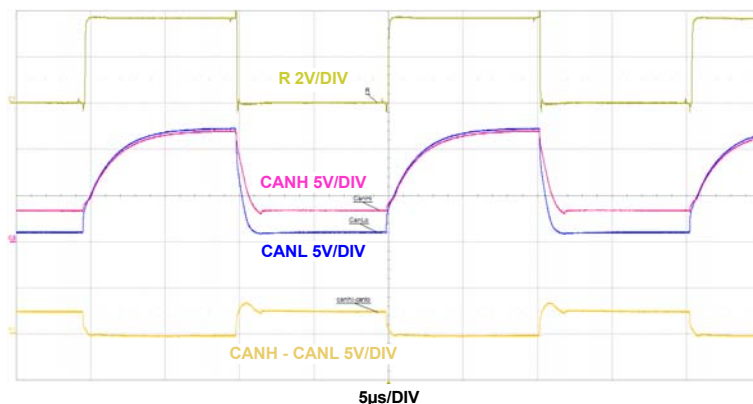


FIGURE 3. Example of CANH/CANL switching at 50kHz, $V_{CC} = 3.6\text{V}$, and a common-mode of $+12\text{V}$. Time allows recessive state to stabilize at $+12\text{V}$ for the CANH/CANL lines. Time scale is $5\mu\text{s}/\text{Div}$, and the vertical axis is $2\text{V}/\text{Div}$ for the upper plot and $5\text{V}/\text{Div}$ for the lower three plots.

TABLE 1. MONITOR MEASUREMENTS AND CONDITIONS FOR SEB DETECTION

MEASUREMENTS MADE	ELECTRICAL CONDITIONS FOR MEASUREMENT									
	RS (V)	D	V _{CC} (V)	V _R (V)	K1	K2	V _{CM} (V)	CANH	CANL	R
I _{CM} (μA) at V _{CM} = -7V	0	4.5	3.6	OP	CL	OP	-7	CH2	CH3	OP
I _{CM} (μA) at V _{CM} = +12V	0	4.5	3.6	OP	CL	OP	+12	CH2	CH3	OP
VREF at V _{CM} (V)	0	4.5	3.6	OP	OP	CL	Meas. V _{REF}	CH2	CH3	OP
I _{CC} (mA) Dynamic Unloaded	0	0V to 4.5V 250kHz	3.6	OP	OP	OP	OP	CH2	CH3	OP
I _{CC} (mA) Dynamic Loaded Slow	OP	0V to 4.5V 250kHz	3.6	1.7V	CL	CL	OP	CH2	CH3	OP
Scope Capture Loaded Slow, 2μs/Div	OP	0V to 4.5V 250kHz, CH1	3.6	1.7V	CL	CL	OP	CH2	CH3	CH4

NOTE: OP = Open and CL = Closed. Measurements of these parameters were made at the start and end of the six SEB tests listed in Table 2. Oscilloscope channels are indicated by "CH".

TABLE 2. SEB TESTS RUN ON ISL72027 DURING THE MARCH 2015 TESTING

	RS (V)	D	V _{CC} (V)	K1	K2	V _{CM} (V)
Cold Spare -18V _{CM}	0	0V to 4.5V 50kHz	0	CL	CL	-18
Cold Spare +18V _{CM}	0	0V to 4.5V 50kHz	0	CL	CL	+18
Fast Op -18V _{CM}	0	0V to 4.5V 50kHz	4.5	CL	OP	-18
Fast Op +18V _{CM}	0	0V to 4.5V 50kHz	4.5	CL	OP	+18
Slow Op -18V _{CM}	OP	0V to 4.5V 50kHz	4.5	CL	CL	-18
Slow Op +18V _{CM}	OP	0V to 4.5V 50kHz	4.5	CL	CL	+18

TABLE 3. SUPPLY CURRENT MONITORS I_{CC} AND I_{CM} FOR EACH IRRADIATION WITH Pr AT 10° FOR LET of 60MeV • cm²/mg TO 5x10⁶ Ion/cm² FOR EACH IRRADIATION.

IRRADIATION CONDITION V _{CC} = 4.5V		DUT1		DUT2		DUT3		DUT4	
		I _{CC} (mA)	I _{CM} (mA)	I _{CC} (mA)	I _{CM} (mA)	I _{CC} (mA)	I _{CM} (mA)	I _{CC} (mA)	I _{CM} (mA)
Cold Spare V _{CM} = -18V	Pre		0.0076		0.0075		0.0075		0.0075
	Post		0.0075		0.0073		0.0075		0.0075
Cold Spare V _{CM} = +18V	Pre		0.0075		0.0077		0.0075		0.0075
	Post		0.0075		0.0076		0.0074		0.0075
Fast Op V _{CM} = +18VN	Pre	3.24	7.85	3.67	8.39	3.26	8.16	3.7	7.48
	Post	3.25	7.83	3.65	8.40	3.246	8.22	3.69	7.49
Fast Op V _{CM} = -18V	Pre	13.01	9.26	14.53	10.37	14.17	10.43	13.26	9.10
	Post	13.16	9.31	14.53	10.39	14.14	10.39	13.27	9.11
Slow Op V _{CM} = -18V	Pre	8.08	4.88	8.61	5.00	8.39	5.21	8.72	5.05
	Post	8.08	4.89	8.61	5.01	8.4	5.22	8.72	5.05
Slow Op V _{CM} = +18V	Pre	3.36	51.07	3.71	52.35	3.48	52.60	3.76	54.00
	Post	3.33	51.80	3.72	52.5	3.38	52.09	3.74	53.53

TABLE 4. SUPPLY CURRENT MONITOR DELTAS (I_{CC} AND I_{CM}) FOR EACH IRRADIATION WITH Pr AT 10° FOR LET OF $60\text{MeV} \cdot \text{cm}^2/\text{mg}$ TO $5 \times 10^6 \text{ion}/\text{cm}^2$ FOR EACH IRRADIATION.

IRRADIATION CONDITION $V_{CC} = 4.5\text{V}$	DUT1		DUT2		DUT3		DUT4	
	I_{CC} DELTA%	I_{CM} DELTA%	I_{CC} DELTA%	I_{CM} DELTA%	I_{CC} DELTA%	I_{CM} DELTA%	I_{CC} DELTA%	I_{CM} DELTA%
Cold Spare -18V_{CM}		-1		-3		0		0
Cold Spare $+18\text{V}_{CM}$		0		-1		-1		0
Fast Op $+18\text{V}_{CM}$	0	0	-1	0	0	1	0	0
Fast Op -18V_{CM}	1	1	0	0	0	0	0	0
Slow Op -18V_{CM}	0	0	0	0	0	0	0	0
Slow Op $+18\text{V}_{CM}$	-1	1	0	0	-3	-1	-1	-1

TABLE 5. PARAMETRIC MONITORS FOR EACH SET OF IRRADIATIONS

		I_{CM} (μA) AT $V_{CM} = -7\text{V}$	I_{CM} (μA) AT $V_{CM} = +12\text{V}$	V_{REF} AT V_{CM} (V)	I_{CC} (mA) UNLOADED FAST	I_{CC} (mA) LOADED SLOW
DUT1	Pre	608	652	1.773	4.11	24.10
	Post	604	649	1.772	4.10	24.05
DUT2	Pre	604	652	1.769	4.51	24.38
	Post	600	649	1.768	4.51	24.45
DUT3	Pre	598	645	1.773	4.11	24.90
	Post	600	644	1.775	4.12	25.14
DUT4	Pre	609	657	1.772	4.55	25.05
	Post	611	656	1.774	4.54	25.11

NOTE: Refer to [Table 2 on page 4](#). Irradiation was with Pr at 10° incidence for effective LET of $60\text{MeV} \cdot \text{cm}^2/\text{mg}$ and each set of irradiations having a total of $3 \times 10^7 \text{ion}/\text{cm}^2$.

TABLE 6. DELTAS OF PARAMETRIC MONITORS FOR EACH SET OF IRRADIATIONS

	I_{CM} (μA) AT $V_{CM} = -7\text{V}$ (%)	I_{CM} (μA) AT $V_{CM} = +12\text{V}$ (%)	V_{REF} AT V_{CM} (V%)	I_{CC} (mA) UNLOADED FAST (%)	I_{CC} (mA) LOADED SLOW (%)
DUT1	-1	0	0	0	0
DUT2	-1	0	0	0	0
DUT3	0	0	0	0	1
DUT4	0	0	0	0	0

NOTE: Refer to [Table 2 on page 4](#). Irradiation was with Pr at 10° incidence for effective LET of $60\text{MeV} \cdot \text{cm}^2/\text{mg}$ and each set of irradiations having $3 \times 10^7 \text{ion}/\text{cm}^2$.

[Tables 5](#) and [6](#) present the collected data for the parameters of [Table 1 on page 4](#) across the irradiation sets. Again, no change was noted that indicated permanent damage to the parts.

It was deduced from the above testing that the ISL72027SEH was found to be free from destructive SEE effects from ions with effective LET of $60\text{MeV} \cdot \text{cm}^2/\text{mg}$ while biased at $V_{CC} = 4.5\text{V}$ and $V_{CM} = \pm 18\text{V}$.

SET Testing of the ISL72027SEH CAN Transceiver at Ag (LET = 43MeV • cm²/mg)

Testing for Single Event Transients (SET) was carried out using silver (Ag) at 1.634GeV for a surface LET = 43MeV • cm²/mg. Beam time constraints on the trip limited the testing to only two units. A summary of the conditions tested and the resulting SET counts appear in [Table 7](#). Examples of the SET captured in the irradiation runs appear in [Figures 4](#) through [7](#).

Stand-alone errant recessive bits of approximately 2μs duration at 43MeV • cm²/mg, as well as spike recessive events are shown in [Figure 4, on page 7](#). These occurred for the bus VOD biased externally at the receiver dominant threshold of 0.9V.

The events in [Figure 5, on page 7](#) are errant dominant spikes occurring on the R output, either with or without concomitant disruption on the VOD signal. In these cases, the bus VOD was externally biased to 0.5V, the receiver recessive threshold. When disturbances on VOD were noted, the erroneous dominant spikes generally came in pairs as on the left side to [Figure 5](#), following the ringing on VOD.

The dynamic testing was done by providing a square wave input to the D pin (0V to 3V) and monitoring the response of the

receiver R pin signal. When the transceiver was set to the slow slew rating of the transmitter, a frequency of 250kHz was used. When the transceiver was set for fast slewing of the transmitter, a 500kHz signal was used, except in the two inadvertent cases of lines eleven and twelve of [Table 7](#).

[Figures 6](#) and [7](#) present examples of the worst dynamic SET that were captured using silver.

The two events represented in the top of [Figure 6, on page 8](#) have clear disturbances on VOD associated with the disruption of the bit stream on R. As with the static tests, these appear to be transmitter SET that are simply reflected in the receiver output. The bottom event in [Figure 6](#) is not clearly associated with a VOD disturbance, however, it certainly occurs during a VOD transition and at the received bit edge. Again, a transmitter SET seems to be indicated.

For the high speed events in [Figure 7, on page 9](#), each SET on R is accompanied by what appears to be a precipitating SET on the VOD signal. Thus, these are all consistent with transmitter events and not receiver SET.

TABLE 7. STATIC CAPTURES AND DYNAMIC SET CAPTURES

TEST CONDITIONS	DUT1 EVENTS	DUT2 EVENTS	DUT2 TOTAL EVENTS	NET CROSS SECTION (cm ²)
VOD Dominant V _{THR} 0.9V	18	14	32	8.0x10 ⁻⁶
VOD Recessive V _{THF} 0.5V	42	51	93	2.3x10 ⁻⁵
Listen only, VOD Dominant V _{THR} 1.05V	0	0	0	-
Listen only, VOD Recessive V _{THF} 0.65V	0	0	0	-
Transmit Slow 250kHz Open CM and V _{REF}	9	14	23	5.8x10 ⁻⁶
Transmit Slow 250kHz Open CM	13	15	28	7.0x10 ⁻⁶
Transmit Slow 250kHz -7V _{CM} and V _{REF}	21	16	37	9.3x10 ⁻⁶
Transmit Slow 250kHz -7V _{CM}	17	15	32	8.0x10 ⁻⁶
Transmit Slow 250kHz +12V _{CM} and V _{REF}	10	6	16	4.0x10 ⁻⁶
Transmit Slow 250kHz +12V _{CM}	5	4	9	2.3x10 ⁻⁶
Transmit Slow 500kHz Open CM and V _{REF}	83	87	170	4.3x10 ⁻⁵
Transmit Slow 500kHz Open CM	95	76	171	4.3x10 ⁻⁵
Transmit Fast 500kHz -7V _{CM} and V _{REF}	12	4	16	4.0x10 ⁻⁶
Transmit Fast 500kHz -7V _{CM}	2	7	9	2.3x10 ⁻⁶
Transmit Fast 500kHz +12V _{CM} and V _{REF}	2	2	4	1.0x10 ⁻⁶
Transmit Fast 500kHz +12V _{CM}	1	4	5	1.3x10 ⁻⁶

NOTE: Static captures were for any change of R state, while dynamic captures were taken for R duty cycle outside of 40% to 60%. The irradiations were with Ag at normal incidence for an LET = 43MeV • cm²/mg and the device at ambient temperature (~25°C). A fluence of 2x10⁶ions/cm² was done for each irradiation.

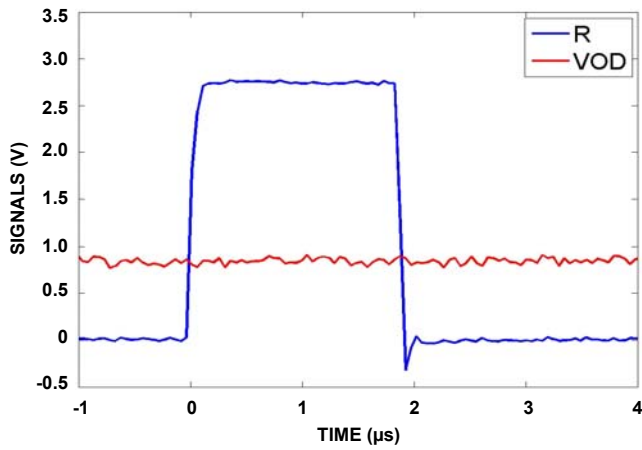


FIGURE 4A.

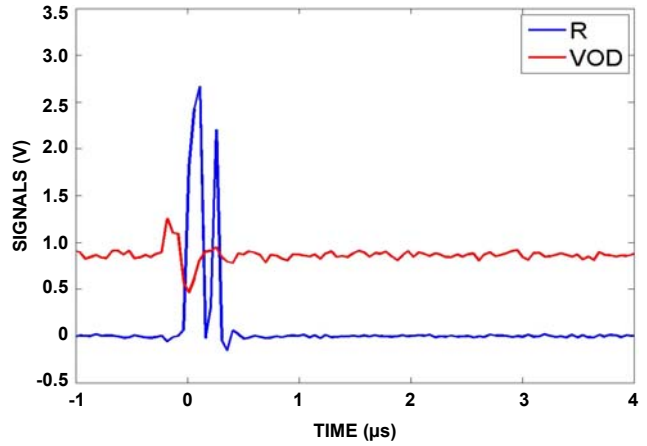


FIGURE 4B.

FIGURE 4. The left-hand SET (Figure 4A) goes from dominant to recessive with no apparent SET on VOD (5/32 IN 4×10^6 FLUENCE). The case on the right (Figure 4B) shows recessive spikes along with a disturbance on VOD and accounted for 27/32 events captured in 4×10^6 fluence.

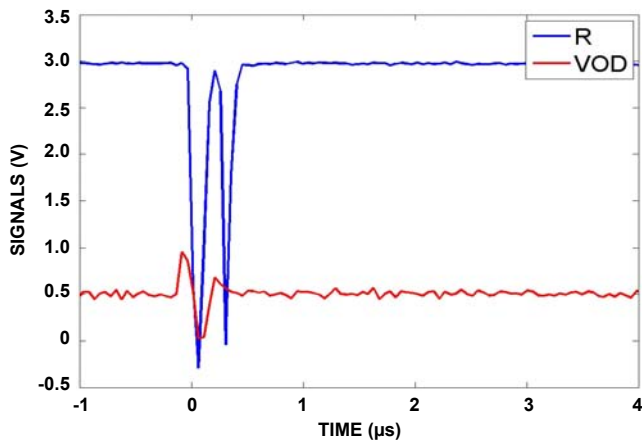


FIGURE 5A.

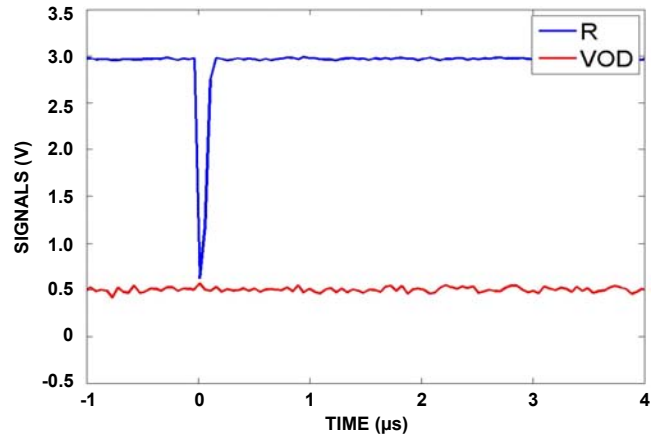


FIGURE 5B.

FIGURE 5. The left-hand SET (Figure 5A) shows dominant spikes in R along with an SET on VOD (17/93). In the right-hand case (Figure 5B), a single dominant spike is unaccompanied by any discernable VOD SET (76/93). The fluence is 4×10^6 .

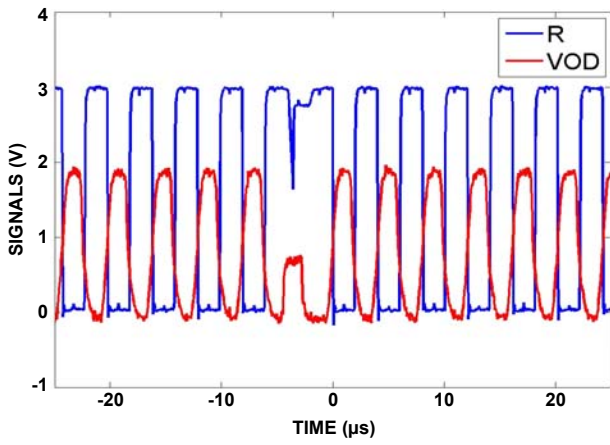


FIGURE 6A. TRANSMIT SLOW OPEN CM

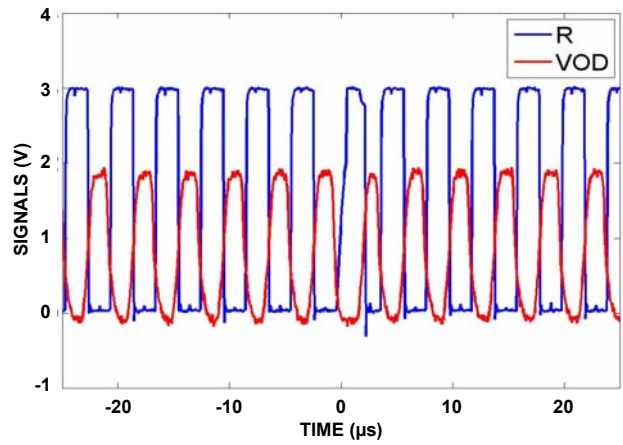


FIGURE 6B. TRANSMIT SLOW OPEN CM AND V_{REF}

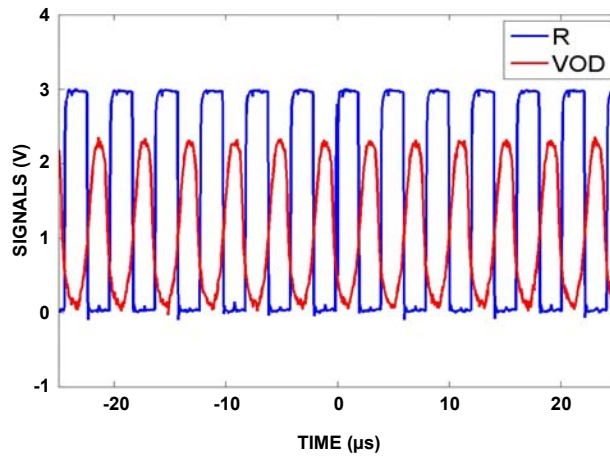


FIGURE 6C. TRANSMIT SLOW $-7V_{CM}$ AND V_{REF}

FIGURE 6. The longest recessive event is in the upper left (transmit slow open CM) and the longest dominant event is in the upper right (transmit slow open CM and V_{REF}). The bottom capture shows a glitch at the leading edge of a recessive bit (transmit slow $-7V_{CM}$ AND V_{REF}).

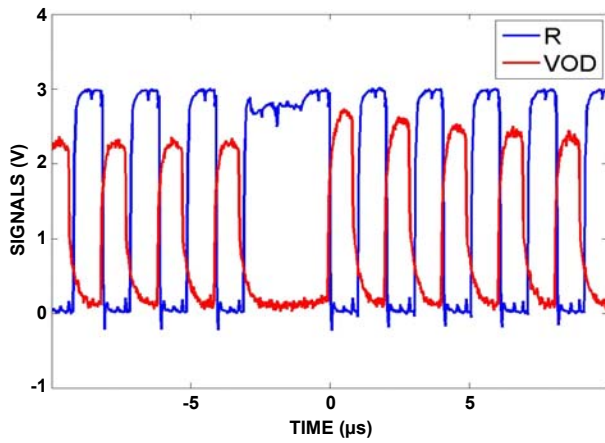


FIGURE 7A. TRANSMIT FAST -7V_{CM} AND V_{REF}

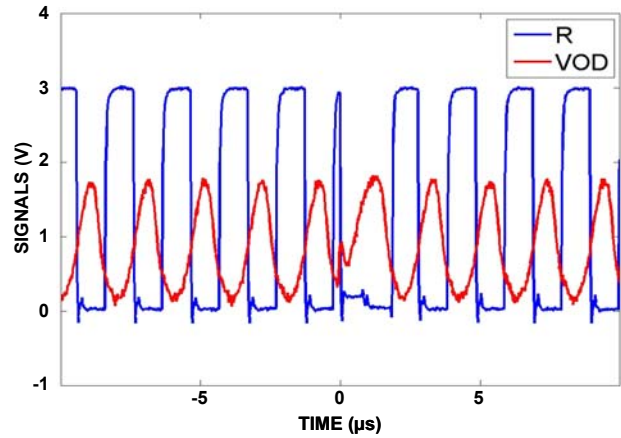


FIGURE 7B. TRANSMIT FAST OPEN CM

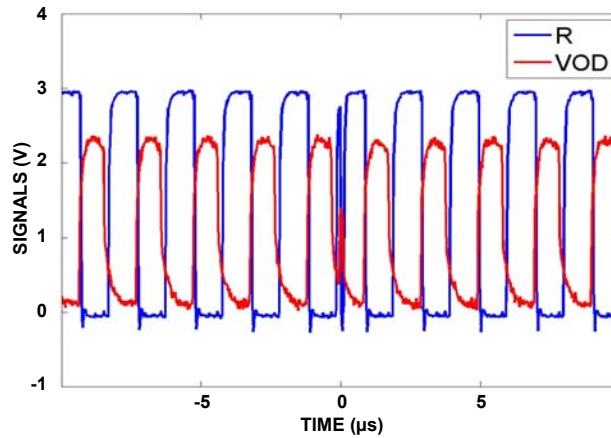


FIGURE 7C. TRANSMIT FAST -7V_{CM} AND V_{REF}

FIGURE 7. The upper left (Figure 7A) shows the longest recessive time (transmit fast -7V_{CM} and V_{REF}). The upper right (Figure 7B) shows the longest dominant time (transmit fast open CM). The lower capture (Figure 7C) shows a dominant spike during a recessive bit (transmit fast -7V_{CM} AND V_{REF}). The plot at upper right (Figure 7B) indicates that the transition speed was not actually set to the high speed setting.

SET Testing of the ISL72027SEH CAN Transceiver at Cu (LET = 20MeV • cm²/mg)

Since SET occurred for LET = 43MeV • cm²/mg, tests were run at the lower LET = 20MeV • cm²/mg using copper. The biasing conditions run were restricted to exclude common-mode biasing cases since, in the higher LET testing, the common-mode conditions did not substantially influence the SET observations. The tests run and the event counts appear in [Table 8](#) while examples of the worst SET observed follow in [Figures 8](#) through [10](#).

In the case of [Figure 8, on page 11](#), the SETs on R are all associated with preceding disturbances on VOD that indicate an SET to the transmitter that impacts the VOD. In these cases, the SET on R is a response to a transmitter SET and not a receiver SET. The ringing on VOD is certainly the result of the cabling used to monitor the VOD voltage. In total, the cross section of these events on four parts is approximately 3.22x10⁻⁶cm².

[Figure 9, on page 11](#) looks at dominant SET occurring when the bus is biased at the recessive threshold of 0.5V. In this case, two distinct types of SET seem to occur. The first is a double spike with a preceding disturbance on the bus (VOD). This would appear to be a transmitter SET that is simply reflected in the receiver output. The second case is a single dominant spike that does not appear to be associated with any real disturbance on the bus (VOD). This would appear to be a genuine receiver SET. Both types of events disappear when the bus is left open rather than being biased to the recessive threshold value.

[Figure 10, on page 12](#) looks at the worst SET occurring with a dynamic bit stream being transmitted with no common-mode. The first two plots are for a 250kHz input signal (500kbit/s alternating 1's and 0's) with slow bus transitions while the third plot is for 500kHz with fast transitions selected. The only events recorded on R were dominant glitches associated with the edges of the bits when the bus (VOD) was in a transition. The SET were all associated with distortions on the VOD waveform and so are believed to originate in the transmitter.

TABLE 8. SET TESTING AT LET = 20MeV • cm²/mg AND FLUENCE OF 1x10⁷Ion/cm² FOR EACH RUN

TEST CONDITIONS	DUT1 EVENTS	DUT2 EVENTS	DUT3 EVENTS	DUT4 EVENTS	CROSS SECTION (cm ²)
VOD Dominant at 1V	20	32	38	39	3.2x10 ⁻⁶
VOD Dominant V _{THR} 0.9V	38	45			4.2x10 ⁻⁶
VOD Recessive V _{THF} 0.5V	65	47	71	78	6.5x10 ⁻⁶
Transmit Dominant Open CM	0	0			-
Transmit Recessive Open CM	0	0			-
Transmit Slow (250kHz) Open CM	13	10	3	9	8.8x10 ⁻⁷
Transmit Fast (500kHz) Open CM	362*	85*	3	4	3.5x10 ⁻⁷

NOTE: The runs marked with an asterisk (*) were accidentally run at slow transition speeds but at higher data rate; this accounts for the higher event counts.

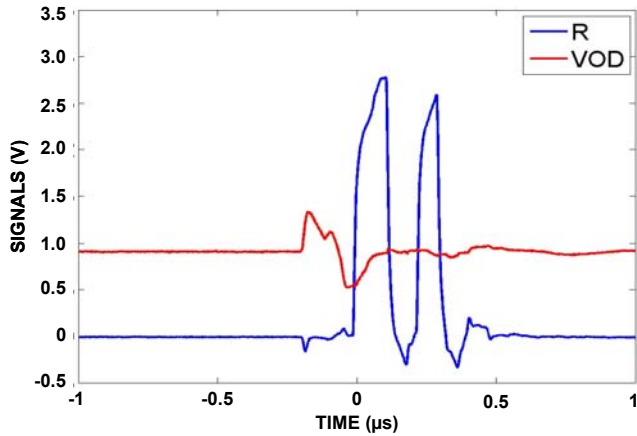


FIGURE 8A.

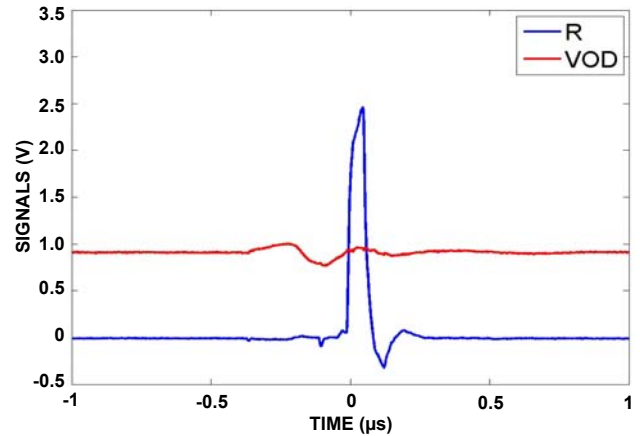


FIGURE 8B.

FIGURE 8. Examples of dominant to recessive set for a dominant threshold (0.9V) on the bus. For DUT1, the double spikes on the left plot (Figure 8A) represented 21/38 events; the single spikes on the right (Figure 8B) represented the other 17/38 events. The total fluence at LET = 20MeV • cm²/mg was 1x10⁷ion/cm². For all events, the SET on VOD preceded the set on R.

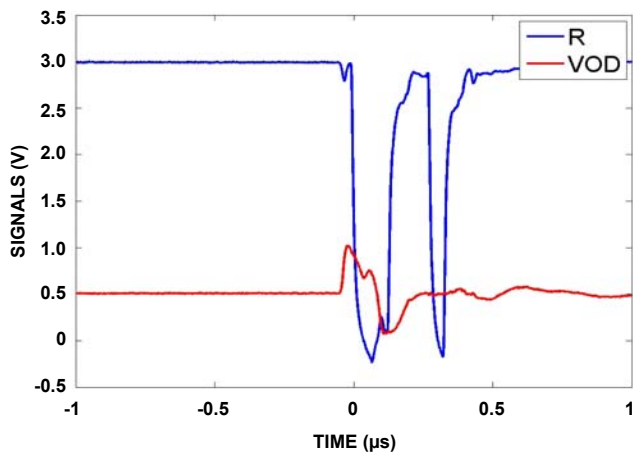


FIGURE 9A.

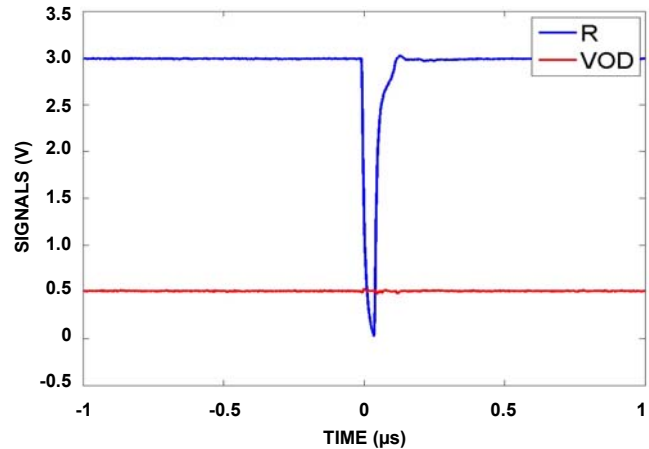


FIGURE 9B.

FIGURE 9. Examples of recessive to dominant set from DUT1 for recessive threshold (0.5V) on the bus. The double spikes on the left plot (Figure 9A) represented 21/65 events; the single spikes on the right (Figure 9B) represented the other 44/65 events. The total fluence per run at LET = 20MeV • cm²/mg was 1x10⁷cm². Only the double spikes on the left showed clear VOD set preceding the R set. The single spikes appear not to have an associated VOD event.

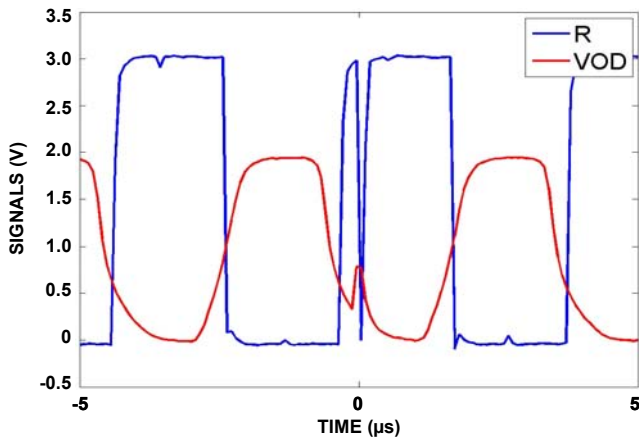


FIGURE 10A.

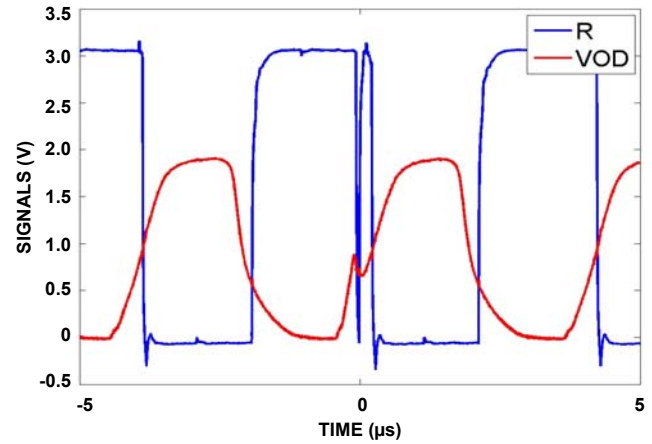


FIGURE 10B.

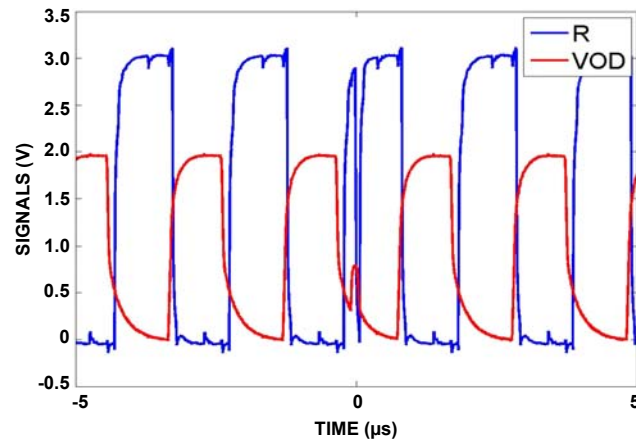


FIGURE 10C.

FIGURE 10. Examples of SET during data transmission. The top events (Figures 10A and 10B) are for slow transmission (DUT1 and DUT2) and the bottom (Figure 10C) is fast transmission (DUT3). The set exhibit VOD transients during transition that result in false dominant SET on the R output. The total fluence per run at LET = 20MeV \cdot cm²/mg was 1×10^7 cm². The top plots (Figures 10A and 10B) indicate that SET can occur on either transition of the VOD. Unlike results at LET = 43MeV \cdot cm²/mg, there were no missing bits of either state.

SET Testing of the ISL72027SEH CAN Transceiver at LET = 8.5 and 2.7MeV • cm²/mg

SET testing was again done on the ISL72027SEH with Ar (LET = 8.5MeV • cm²/mg) and Ne (LET = 2.7MeV • cm²/mg). With argon, events were only recorded for the case of the bus operating at the dominant threshold of 0.9V and for dynamic operation as represented in Table 9. With neon (2.7MeV • cm²/mg), no SET at all were observed. Again, beam time constraints limited testing to only two units.

For the static SET observed with VOD = 0.9V (dominant threshold), recessive spikes, either single or double spikes, were observed, as depicted in Figure 11. Twenty five of the fifty-eight SET observed were of the double spike variety. All the observed SET began with what appears to be an attempt of the transmitter to assert a dominant state on the CAN bus (rise in VOD) followed by some ringing on the bus that was interpreted by the receiver as being a recessive state. This is consistent with no SET being observed for an applied VOD of 1.5V, where the errant dominant

state would not cause a transient sufficient to result in bus ringing to invoke a recessive state on the receiver.

The dynamic SET were almost non-existent with only four being recorded for the fast slew setting. All four look quite similar and are represented in the top two plots of Figure 12, on page 14. In the first plot (Figure 12A), no apparent disturbance can be discerned in the VOD trace, while in the second plot (Figure 12B), a clear glitch in the VOD trace is evident. In both cases the R transition from dominant to recessive is interrupted by a spike back to dominant. The spikes occur during the transition and are on the order of 100ns in duration. The third SET (bottom of Figure 12C) shows a clear VOD glitch on the slower slew rate transition of the VOD signal.

TABLE 9. RESULTS FOR SET TESTING WITH LET = 8.5MeV • cm²/mg (Ar) TO 1x10⁷ Ion/cm² PER RUN

TEST CONDITIONS	DUT1 EVENTS	DUT2 EVENTS	TOTAL EVENTS	CROSS SECTION (cm ²)
Recessive Xmit Open Bus, High Slew	0	0	0	-
Recessive Xmit Open Bus, Medium Slew	0	0	0	-
Dominant Xmit Open Bus, High Slew	0	0	0	-
Dominant Xmit Open Bus, Medium Slew	0	0	0	-
VCANH = 1.9V, VCANL = 1.0V, High Slew	29	29	58	2.9x10 ⁻⁶
VCANH = 1.9V, VCANL = 1.0V, Medium Slew	31	31	62	3.1x10 ⁻⁶
VCANH = 2.5V, VCANL = 1.0V, High Slew	0	0	0	-
VCANH = 2.5V, VCANL = 1.0V, Medium Slew	0	0	0	-
Transmit 500kHz, Fast, No CM or V _{REF}	4	0	4	2x10 ⁻⁷
Transmit 500kHz, Medium, No CM or V _{REF}	1	0	1	5x10 ⁻⁸

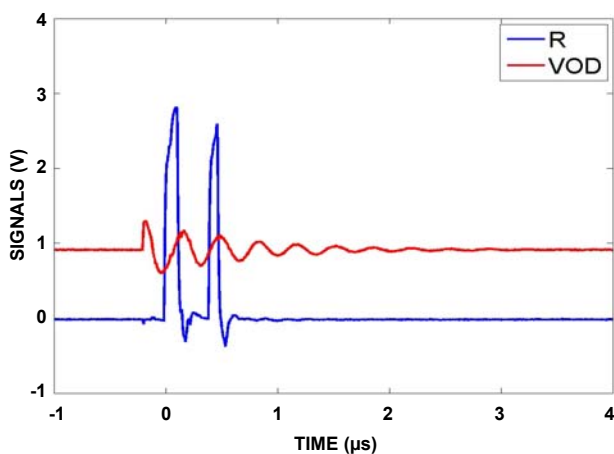


FIGURE 11A.

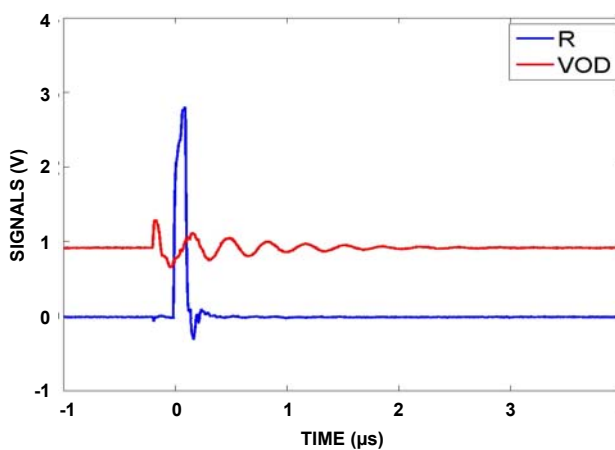


FIGURE 11B.

FIGURE 11. Example SET for LET = 8.5MeV • cm²/mg with VCANH = 1.9V and VCANL = 1V (V_{OD} = 1.5V).

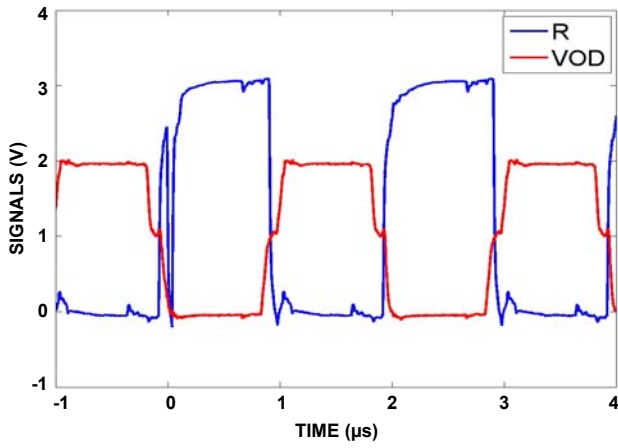


FIGURE 12A.

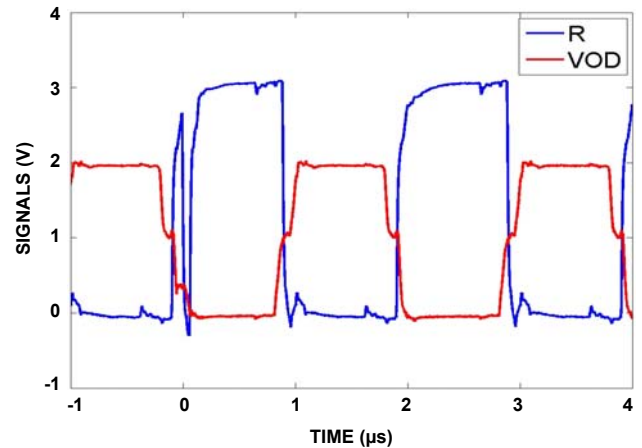


FIGURE 12B.

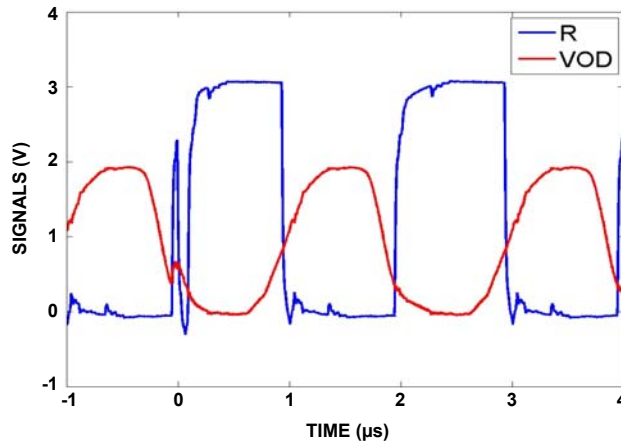


FIGURE 12C.

FIGURE 12. Examples of dynamic SET at LET = 8.5MeV • cm²/mg for fast slew ([Figures 12A and 12B](#)) and for medium slew ([Figure 12C](#)).

Discussion and Conclusions

Damaging SEE

Testing of the ISL72027SEH at case temperatures of +125°C \pm 10°C and 60MeV \cdot cm²/mg did not yield damaging SEE effects with a supply of V_{CC} = 4.5V and the CAN bus common-mode (CANH, CANL) at \pm 18V. The tests were run on four parts to 5x10⁶ ions/cm² on each of six irradiation runs per part, including both polarities of common-mode for cold sparing, and for fast and slow transmitter slewing. Consequently, it is concluded that the part is immune to damaging SEE effects at 60MeV \cdot cm²/mg while operating at or below the voltages of V_{CC} = 4.5V and bus common-mode voltages of \pm 18V.

Single Event Transients

The ISL72027SEH exhibited SET susceptibility at LET = 43, 20, and 8.5MeV \cdot cm²/mg. SET was defined as any transition in the receiver output for static biasing conditions and any received bit outside of 40% to 60% duty-cycle for a 50% transmitted bit stream. No SET of either type were recorded at an LET = 2.7MeV \cdot cm²/mg.

At the higher LET level (43MeV \cdot cm²/mg), SET represented by [Figure 4A, on page 7](#) were noted. The receiver dominant signal was interrupted for nearly 2 μ s by an errant recessive received signal while the bus was being externally biased to 0.9V. This type of SET represented a cross section at 43MeV \cdot cm²/mg of approximately 1.3x10⁻⁶cm². This type of event disappeared at LET = 20MeV \cdot cm²/mg and below.

The form of SET depicted in [Figure 4B](#), a recessive receiver spike or double spike during a dominant bus voltage of 0.9V, occurred for LET down to 8.5MeV \cdot cm²/mg with a cross section down to 3.0x10⁻⁶cm² at that LET. These events disappeared at LET = 2.7MeV \cdot cm²/mg to yield a cross section limit of 5x10⁻⁸ cm².

With the bus externally biased to the recessive threshold of 0.5V, SET consisting of receiver dominant spikes as in [Figure 5, on page 7](#) were noted. Most of these SET correlated to VOD disturbances indicating a transmitter SET as the initiating event, though some of the shortest events were not accompanied by a VOD disturbance. At an LET of 20MeV \cdot cm²/mg, these events had a cross section of 6.5x10⁻⁶cm².

Dynamic testing of the part for SET resulted in missing bits at the receiver as in [Figures 6 and 7 on page 9](#) for 43MeV \cdot cm²/mg. At LET of 20MeV \cdot cm²/mg and below, dynamic testing only resulted in glitches on the transitions of the bits as in [Figures 10 and 12 on page 14](#). At LET of 8.5MeV \cdot cm²/mg, the cross section for this SET was 2.0x10⁻⁷cm². At LET of 2.7MeV \cdot cm²/mg, there were no SET recorded to a nominal 5x10⁻⁸cm².

Subsequent Addendum

Subsequent to the data reported above, some additional testing was undertaken and is reported in the following two Addendum. This extra data is important and should be considered in addition to the data reported above.

June 2016 SET Addendum

On June 25, 2016, another group of SET tests was done to better quantify the SET behavior of the ISL72027SEH under heavy ion irradiation. Four units of the ISL72027SEH were irradiated in pairs at various LET (86, 43, 28, 20, 8.5, and 2.7 MeV • cm²/mg) for both RS = 0Ω (fast bus slew rate) and RS = 10kΩ (medium bus slew rate) operating conditions. The test schematic appears in [Figure 1, on page 2](#). The transmit data (D) was adjusted to yield a 500kHz square wave for a 1.5V criteria on the received signal (R). The received signal was monitored by an oscilloscope and triggered an event capture when the received pulse width deviated by ±50ns or more from the 1μs nominal. The CANH and CANL signals were also monitored by two other oscilloscope channels. The K2 relay was left open so the CANH/L were not provided with VREF.

The SET count results are summarized in [Table 10](#) and [Table 11](#) below. Testing progressed with decreasing LET and was terminated when SET counts of zero resulted for all four DUTs.

The SET data of [Table 10](#) and [Table 11](#) was reduced to Weibull statistics and parametric fits with the results in [Table 12 on page 17](#). The Weibull results were then submitted to CRÈME96 simulation to calculate the SET rates for a geosynchronous orbit of solar minimum conditions. The CRÈME96 run included all species of ions (atomic number or 2-92) with a minimum energy of 0.1MeV/nucleon. Shielding with 100 mils of aluminum was included. The resulting rates, if interpreted as message errors, indicate an error once every 10.7 years worst case.

June 2016 SET Addendum Conclusions

The SET study of June 2016 established that even with using a sensitive criteria of a ±50ns perturbation of a 1Mbps alternating bit stream, the cross section of events is small and represents a very low rate of error occurrence (1 per 10.7 years) under the worst case conditions, medium slew rate. With the fast slew rate selected for the transmitter the error rate dropped to an error every 2000 years.

TABLE 10. ±50ns PULSE WIDTH DEVIATION SET COUNTS FOR 500kHz SIGNAL WITH RS = 0Ω (FAST SLEW) ALONG WITH CROSS SECTIONS AND EXTRAPOLATED ZERO CROSS SECTION LET. EACH IRRADIATION WAS FOR 1x10⁷ Ion/cm² AT 25°C WITH VCC = 3.0V.

LET (SPECIES) MeV-cm ² /mg	500kHz, 50ns SET EVENTS FOR RS = 0Ω, 1x10 ⁷ Ion/cm ²				RESULTING CROSS SECTION (cm ²)			EXTRAPOLATED ZERO CS LET
	DUT1	DUT2	DUT3	DUT4	MIN	MAX	MEAN	
86 (Au)	31	16	46	23	1.6x10 ⁻⁶	4.6x10 ⁻⁶	2.9x10 ⁻⁶	
43 (Ag)	31	8	30	6	6.0x10 ⁻⁷	3.1x10 ⁻⁶	1.9x10 ⁻⁶	-35.7
28 (Kr)	3	0	8	0	0.0	8.0x10 ⁻⁷	2.8x10 ⁻⁷	24.7
20 (Cu)	0	0	0	0	0.0	0.0	0.0	
8.5 (Ar)	-	-	-	-				
2.7 (Ne)	-	-	-	-				

TABLE 11. ±50ns PULSE WIDTH DEVIATION SET COUNTS FOR 500kHz SIGNAL WITH RS = 10kΩ (MEDIUM SLEW) ALONG WITH CROSS SECTIONS AND EXTRAPOLATED ZERO CROSS SECTION LET. EACH IRRADIATION WAS FOR 1x10⁷ Ion/cm² AT 25°C WITH VCC = 3.0V.

LET (SPECIES) MeV-cm ² /mg	500kHz, 50ns SET EVENTS FOR RS = 10kΩ, 1x10 ⁷ Ion/cm ²				RESULTING CROSS SECTION (cm ²)			EXTRAPOLATED ZERO CS LET
	DUT1	DUT2	DUT3	DUT4	MIN	MAX	MEAN	
86 (Au)	1868	2157	2025	1956	1.9x10 ⁻⁴	2.2x10 ⁻⁴	2.0x10 ⁻⁴	
43 (Ag)	1378	990	912	1437	9.1x10 ⁻⁵	1.4x10 ⁻⁴	1.2x10 ⁻⁴	-18.7
28 (Kr)	415	928	867	525	4.2x10 ⁻⁵	9.3x10 ⁻⁵	6.8x10 ⁻⁵	7.3
20 (Cu)	535	275	226	598	2.3x10 ⁻⁵	6.0x10 ⁻⁵	4.1x10 ⁻⁵	8.1
8.5 (Ar)	6	34	39	14	6.0x10 ⁻⁷	3.9x10 ⁻⁶	2.3x10 ⁻⁶	7.8
2.7 (Ne)	0	0	0	0	0.0	0.0	0.0	

TABLE 12. WEIBULL PARAMETER FIT OF THE SET DATA OF Table 10 AND Table 11. THE DATA FITTING WAS DONE ON BOTH THE MEAN (MEAN) SET OCCURRENCES AND THE MAXIMUM (MAX) SET OCCURRENCES FOR BOTH OF THE SLEW RATE OPTIONS. EVENT RATES WERE CALCULATED VIA CRÈME96 FOR A SOLAR MINIMUM GEOSYNCHRONOUS ORBIT AND 100 mil OF ALUMINUM SHIELDING.

WEIBULL PARAMETERS	FAST SLEW		MEDIUM SLEW	
	DATA MEAN	DATA MAX	DATA MEAN	DATA MAX
Onset LET (MeV-cm ² /mg)	20.09	20.00	7.16	7.55
Width LET (MeV-cm ² /mg)	22.50	21.52	48.07	39.95
Exponent	2.21	1.67	1.27	1.10
Saturation Cross Section (μm ²)	290	461	23641	24570
Geosynchronous orbit with and 100 mil Al (events/(day-device))	6.56x10 ⁻⁷	1.37x10 ⁻⁶	1.83x10 ⁻⁴	2.54x10 ⁻⁴

August 2016 SEB Addendum

Subsequent to the previous report, further testing for damaging SEE (referred to as SEB but to include SEL and SEGR) was done on the ISL72027SEH parts on August 27th of 2016. Two major changes were introduced into the testing. First, the testing was done at +25°C ambient rather than +125°C case temperature. Second, the voltages used for testing were increased to $\pm 20V$ for the common-mode voltage to the bus pins and +5.5V on the supply pin VCC when powered.

The ion species used was gold (Au) to yield a surface LET of $86MeV \cdot cm^2/mg$ at a 0° angle of incidence. Each irradiation was taken to a fluence of 1×10^7 ion/cm². Four tests were run on each of four units as described in [Table 13](#).

As done previously, the supply current (I_{CC}) and the bus common-mode current (I_{CM}) were monitored before and after each irradiation and are reported in [Table 14](#). The deltas for I_{CC} and I_{CM} are presented in [Table 15](#). The changes in I_{CC} and I_{CM} do not provide any indication of damage due to the irradiations.

Before and after each grouping of the four tests indicated in [Table 13](#), the monitor parameters as described in [Table 1 on page 4](#) were measured. The raw data for these measurements is provided in [Table 16 on page 19](#). The data reduced to deltas in the parameters across the grouping of four irradiations is presented in [Table 17 on page 19](#). Again the data gives no indication of any damage due to the irradiations.

August 2016 SEB Addendum Conclusions

From this additional testing it is concluded that the ISL72027SEH did not suffer any damage when operated at room temperature with $V_{CC} = 5.5V$ and $V_{CM} = \pm 20V$ and irradiated with ions having LET of $86MeV \cdot cm^2/mg$. The irradiations were carried out with the part at ambient temperature of approximately +25°C and each irradiation was taken to 1×10^7 ion/cm².

TABLE 13. SEB TESTS RUN ON ISL72027 DURING THE AUGUST 2016 TESTING

	RS (V)	D	V _{CC} (V)	K1	K2	V _{CM} (V)
Cold Spare -20V _{CM}	0	0V to 5.5V 50kHz	0	CL	CL	-20
Cold Spare +20V _{CM}	0	0V to 5.5V 50kHz	0	CL	CL	+20
Slow Op -20V _{CM}	OP	0V to 5.5V 50kHz	5.5	CL	CL	-20
Slow Op +20V _{CM}	OP	0V to 5.5V 50kHz	5.5	CL	CL	+20

TABLE 14. SUPPLY AND COMMON-MODE CURRENT MONITOR VALUES FOR SEB IRRADIATIONS AT $V_{CC} = 5.5V$ AND $V_{CM} = \pm 20V$

IRRADIATION CONDITION LET = $86MeV \cdot cm^2/mg$		DUT1		DUT2		DUT3		DUT4	
		I _{CC} (mA)	I _{CM} (mA)	I _{CC} (mA)	I _{CM} (mA)	I _{CC} (mA)	I _{CM} (mA)	I _{CC} (mA)	I _{CM} (mA)
V _{CC} = 0 V _{CM} = -20V	Pre		0.0053		0.0060		0.0063		0.0073
	Post		0.0054		0.0063		0.0062		0.0074
V _{CC} = 0 V _{CM} = +20V	Pre		0.0061		0.0067		0.0065		0.0081
	Post		0.0057		0.0066		0.0061		0.0078
V _{CC} = 5.5V V _{CM} = -20V Slow 50kHz	Pre	7.95	66.98	8.34	67.24	8.86	68.94	8.94	69.04
	Post	7.94	66.68	8.46	68.50	8.03	67.75	8.09	67.98
V _{CC} = 5.5V V _{CM} = +20V Slow 50kHz	Pre	93.86	88.46	95.92	90.82	94.64	89.24	94.75	89.564
	Post	94.36	88.93	96.31	91.26	95.91	90.31	95.10	90.468

TABLE 15. SUPPLY AND COMMON-MODE CURRENT DELTAS FOR SEB IRRADIATIONS AT $V_{CC} = 5.5V$ AND $V_{CM} = \pm 20V$

IRRADIATION CONDITION $V_{CC} = 5.5V$	DUT1		DUT2		DUT3		DUT4	
	I_{CC} DELTA (%)	I_{CM} DELTA (%)	I_{CC} DELTA (%)	I_{CM} DELTA (%)	I_{CC} DELTA (%)	I_{CM} DELTA (%)	I_{CC} DELTA (%)	I_{CM} DELTA (%)
$V_{CC} = 0$ $V_{CM} = -20V$		1.9		5.0		-1.6		1.4
$V_{CC} = 0$ $V_{CM} = +20V$		6.6		-1.5		-6.2		-3.7
$V_{CC} = 5.5V$ $V_{CM} = -20V$ Slow 50kHz	-0.2	-0.4	1.5	-1.9	-9.4	-1.7	-9.5	-1.5
$V_{CC} = 5.5V$ $V_{CM} = +20V$ Slow 50kHz	0.5	0.5	0.4	0.5	1.3	1.2	0.4	1.0

TABLE 16. PARAMETRIC MONITORS FOR EACH SET OF IRRADIATIONS

		I_{CM} (μA) AT $V_{CM} = -7V$	I_{CM} (μA) AT $V_{CM} = +12V$	V_{REF} AT V_{CM} (V)	I_{CC} (mA) UNLOADED FAST	I_{CC} (mA) LOADED SLOW
DUT1	Pre	771	820	1.775	4.068	22.856
	Post	761	812	1.774	4.039	22.617
DUT2	Pre	783	833	1.775	4.448	23.665
	Post	774	830	1.774	4.419	24.514
DUT3	Pre	773	833	1.775	4.327	24.985
	Post	757	824	1.773	4.314	26.506
DUT4	Pre	783	861	1.775	4.359	25.150
	Post	757	853	1.774	4.332	26.821

NOTE: Refer to [Table 13 on page 18](#). Irradiation was with Au at 0° incidence for effective LET of $86MeV \cdot cm^2/mg$ and each SET of irradiations having a total of $4 \times 10^7 ion/cm^2$.

TABLE 17. DELTAS OF PARAMETRIC MONITORS FOR EACH SET OF IRRADIATIONS

	I_{CM} (μA) AT $V_{CM} = -7V$ (%)	I_{CM} (μA) AT $V_{CM} = +12V$ (%)	V_{REF} AT V_{CM} (V) (%)	I_{CC} (mA) UNLOADED FAST (%)	I_{CC} (mA) LOADED SLOW (%)
DUT1	-1.3	-1.0	-0.1	-0.7	-1.0
DUT2	-1.1	-0.4	-0.1	-0.7	3.6
DUT3	-2.1	-1.1	-0.1	-0.3	6.1
DUT4	-3.3	-0.9	-0.1	-0.6	6.6

NOTE: Refer to [Table 13 on page 18](#). Irradiation was with Au at 0° incidence for effective LET of $86MeV \cdot cm^2/mg$ and each SET of irradiations having $4 \times 10^7 ion/cm^2$.

Notice

1. Descriptions of circuits, software and other related information in this document are provided only to illustrate the operation of semiconductor products and application examples. You are fully responsible for the incorporation or any other use of the circuits, software, and information in the design of your product or system. Renesas Electronics disclaims any and all liability for any losses and damages incurred by you or third parties arising from the use of these circuits, software, or information.
2. Renesas Electronics hereby expressly disclaims any warranties against and liability for infringement or any other claims involving patents, copyrights, or other intellectual property rights of third parties, by or arising from the use of Renesas Electronics products or technical information described in this document, including but not limited to, the product data, drawings, charts, programs, algorithms, and application examples.
3. No license, express, implied or otherwise, is granted hereby under any patents, copyrights or other intellectual property rights of Renesas Electronics or others.
4. You shall not alter, modify, copy, or reverse engineer any Renesas Electronics product, whether in whole or in part. Renesas Electronics disclaims any and all liability for any losses or damages incurred by you or third parties arising from such alteration, modification, copying or reverse engineering.
5. Renesas Electronics products are classified according to the following two quality grades: "Standard" and "High Quality". The intended applications for each Renesas Electronics product depends on the product's quality grade, as indicated below.
"Standard": Computers; office equipment; communications equipment; test and measurement equipment; audio and visual equipment; home electronic appliances; machine tools; personal electronic equipment; industrial robots; etc.
"High Quality": Transportation equipment (automobiles, trains, ships, etc.); traffic control (traffic lights); large-scale communication equipment; key financial terminal systems; safety control equipment; etc.
Unless expressly designated as a high reliability product or a product for harsh environments in a Renesas Electronics data sheet or other Renesas Electronics document, Renesas Electronics products are not intended or authorized for use in products or systems that may pose a direct threat to human life or bodily injury (artificial life support devices or systems; surgical implantations; etc.), or may cause serious property damage (space system; undersea repeaters; nuclear power control systems; aircraft control systems; key plant systems; military equipment; etc.). Renesas Electronics disclaims any and all liability for any damages or losses incurred by you or any third parties arising from the use of any Renesas Electronics product that is inconsistent with any Renesas Electronics data sheet, user's manual or other Renesas Electronics document.
6. When using Renesas Electronics products, refer to the latest product information (data sheets, user's manuals, application notes, "General Notes for Handling and Using Semiconductor Devices" in the reliability handbook, etc.), and ensure that usage conditions are within the ranges specified by Renesas Electronics with respect to maximum ratings, operating power supply voltage range, heat dissipation characteristics, installation, etc. Renesas Electronics disclaims any and all liability for any malfunctions, failure or accident arising out of the use of Renesas Electronics products outside of such specified ranges.
7. Although Renesas Electronics endeavors to improve the quality and reliability of Renesas Electronics products, semiconductor products have specific characteristics, such as the occurrence of failure at a certain rate and malfunctions under certain use conditions. Unless designated as a high reliability product or a product for harsh environments in a Renesas Electronics data sheet or other Renesas Electronics document, Renesas Electronics products are not subject to radiation resistance design. You are responsible for implementing safety measures to guard against the possibility of bodily injury, injury or damage caused by fire, and/or danger to the public in the event of a failure or malfunction of Renesas Electronics products, such as safety design for hardware and software, including but not limited to redundancy, fire control and malfunction prevention, appropriate treatment for aging degradation or any other appropriate measures. Because the evaluation of microcomputer software alone is very difficult and impractical, you are responsible for evaluating the safety of the final products or systems manufactured by you.
8. Please contact a Renesas Electronics sales office for details as to environmental matters such as the environmental compatibility of each Renesas Electronics product. You are responsible for carefully and sufficiently investigating applicable laws and regulations that regulate the inclusion or use of controlled substances, including without limitation, the EU RoHS Directive, and using Renesas Electronics products in compliance with all these applicable laws and regulations. Renesas Electronics disclaims any and all liability for damages or losses occurring as a result of your noncompliance with applicable laws and regulations.
9. Renesas Electronics products and technologies shall not be used for or incorporated into any products or systems whose manufacture, use, or sale is prohibited under any applicable domestic or foreign laws or regulations. You shall comply with any applicable export control laws and regulations promulgated and administered by the governments of any countries asserting jurisdiction over the parties or transactions.
10. It is the responsibility of the buyer or distributor of Renesas Electronics products, or any other party who distributes, disposes of, or otherwise sells or transfers the product to a third party, to notify such third party in advance of the contents and conditions set forth in this document.
11. This document shall not be reprinted, reproduced or duplicated in any form, in whole or in part, without prior written consent of Renesas Electronics.
12. Please contact a Renesas Electronics sales office if you have any questions regarding the information contained in this document or Renesas Electronics products.
(Note 1) "Renesas Electronics" as used in this document means Renesas Electronics Corporation and also includes its directly or indirectly controlled subsidiaries.
(Note 2) "Renesas Electronics product(s)" means any product developed or manufactured by or for Renesas Electronics.

(Rev.4.0-1 November 2017)



SALES OFFICES

Renesas Electronics Corporation

<http://www.renesas.com>

Refer to "<http://www.renesas.com/>" for the latest and detailed information.

Renesas Electronics America Inc.
1001 Murphy Ranch Road, Milpitas, CA 95035, U.S.A.
Tel: +1-408-432-8888, Fax: +1-408-434-5351

Renesas Electronics Canada Limited
9251 Yonge Street, Suite 8309 Richmond Hill, Ontario Canada L4C 9T3
Tel: +1-905-237-2004

Renesas Electronics Europe Limited
Dukes Meadow, Millboard Road, Bourne End, Buckinghamshire, SL8 5FH, U.K
Tel: +44-1628-651-700, Fax: +44-1628-651-804

Renesas Electronics Europe GmbH
Arcadiastrasse 10, 40472 Düsseldorf, Germany
Tel: +49-211-6503-0, Fax: +49-211-6503-1327

Renesas Electronics (China) Co., Ltd.
Room 1709 Quantum Plaza, No.27 ZhichunLu, Haidian District, Beijing, 100191 P. R. China
Tel: +86-10-8235-1155, Fax: +86-10-8235-7679

Renesas Electronics (Shanghai) Co., Ltd.
Unit 301, Tower A, Central Towers, 555 Langao Road, Putuo District, Shanghai, 200333 P. R. China
Tel: +86-21-2226-0888, Fax: +86-21-2226-0999

Renesas Electronics Hong Kong Limited
Unit 1601-1611, 16/F., Tower 2, Grand Century Place, 193 Prince Edward Road West, Mongkok, Kowloon, Hong Kong
Tel: +852-2265-6688, Fax: +852-2886-9022

Renesas Electronics Taiwan Co., Ltd.
13F, No. 363, Fu Shing North Road, Taipei 10543, Taiwan
Tel: +886-2-8175-9600, Fax: +886-2-8175-9670

Renesas Electronics Singapore Pte. Ltd.
80 Bendemeer Road, Unit #06-02 Hyflux Innovation Centre, Singapore 339949
Tel: +65-6213-0200, Fax: +65-6213-0300

Renesas Electronics Malaysia Sdn.Bhd.
Unit 1207, Block B, Menara Amcorp, Amcorp Trade Centre, No. 18, Jln Persiaran Barat, 46050 Petaling Jaya, Selangor Darul Ehsan, Malaysia
Tel: +60-3-7955-9390, Fax: +60-3-7955-9510

Renesas Electronics India Pvt. Ltd.
No.777C, 100 Feet Road, HAL 2nd Stage, Indiranagar, Bangalore 560 038, India
Tel: +91-80-67208700, Fax: +91-80-67208777

Renesas Electronics Korea Co., Ltd.
17F, KAMCO Yangjae Tower, 262, Gangnam-daero, Gangnam-gu, Seoul, 06265 Korea
Tel: +82-2-558-3737, Fax: +82-2-558-5338